Delay Cournot Duopoly Models Revisited*

Luca Guerrini† Akio Matsumoto‡ Ferenc Szidarovszky§

Abstract

In considering economic dynamics, it has been known that time delays are inherent in economic phenomena and could be crucial sources for oscillatory behavior. The main aim of this study is to shed light on what effects the delays can generate. To this end, different models of Cournot duopoly with different delays are build in a continuous time framework and their local and global dynamics are analytically and numerically examined. Three major findings are obtained. First, the stability switching conditions are analytically constructed. Second, it is numerically demonstrated that different length of the delays are sources for the birth of simple and complicated dynamics. Third, the delay for collecting information on the competitors' output alone does not affect stability.

Keywords: Implementation delay, Information delay, Cournot duopoly, Stability switching curve, Dual roles, Bifurcation diagram

*All authors acknowledge the helpful comments and constructive suggestions from two anonymouse referees. The usual disclaimers apply.

†Department of Management, Polytechnic University of Marche, 60121 Ancona, Italy. luca.guerrini@univpm.it

‡Department of Economics, Chuo University, 742-1, Higashi-Nakano, Hachioji, Tokyo 192-0393, Japan. akiom@tamacc.chuo-u.ac.jp

§Department of Applied Mathematics, University of Pécs, Ifjúság u 6, 7624 Pécs, Hungary. szidarka@gmail.com

1 Introduction

This paper reconsiders the stability conditions of the delay Cournot oligopoly models studied by Howroyd and Russel (1984) ("HR" henceforth). Constructing n-firm Cournot oligopoly models in a continuous-time framework, HR provides a sufficient condition for stability under circumstances in which each firm experiences delays in implementing information on its own output (i.e., implementation delay) and in collecting information on its competitors' outputs (i.e., information delay). Further, HR shows that the information delays do not affect stability when each firm has instantaneous knowledge on its own output. Based on these results, we move one step forward and investigate a sufficient and necessary condition for stability. To simplify the complicated problem, we draw attention only to a Cournot duopoly in this study.

Oligopoly theory has a long history since the pioneering work of Cournot (1838). Its stability properties are first investigated by Theocharis (1960). It is shown that only the number of the firms involved in a market determines stability of a linear Cournot oligopoly in a discrete-time framework: the steady state is stable in the duopoly, marginal stable in the triopoly and unstable if the number is more than three. McManus and Quandt (1961) and Hahn (1962) prove asymptotically stability in the continuous-time adjustment process with demand and cost functions having the appropriate slopes. Okuguchi (1976) summarizes the early results on static and dynamic oligopolies. Okuguchi and Szidarovszky (1999) discuss their multiproduct generalization. During the last two decades, an increasing attention has been given mainly to discrete-time nonlinear dynamics. Bischi et al. (2010) give a comprehensive summary of the newer developments. However, in most of these models the availability of instantaneous information was assumed to the firms about the actions of the competitors. Data collection about the compatitors needs time, and then finding optimal decisions and implementing them are additional reasons why the firms use delayed information on the actions of the competitors and also on their own decision variables. If discrete time scales are selected, then the delays are assumed to be positive integers, so the delay models can be rewritten as higher dimensional models without delays. In the continuous case delay differential equations are used. As the same as an ordinary differential equation, the stability of a delay differential equation depends on the location of the roots of the associated characteristic equation. In consequence, the roots are functions of delays and thus the stability may change as the length of delay changes. Such phenomena are referred to as *stability switches*. For differential equations with one delay, Cooke and Grossman (1982) improve the key techniques to utilize. However, concerning multi-delay dynamics, it has not been discussed until quite recently. This is because the inclusion of multiple delays in equations makes the detail descriptions of the dynamic process too complicated and in addition, no mathematical methods are available for dealing with such delay dynamic models, although importance of multiple delays inherent in the process of obtaining information has been realized. Only recently, Gu et al. (2005) develop a methodology to construct the stability switching curves in the two-delay models. Based on this work, Lin and Wang (2012) suggest an algorithm for the three delay case. These curves show where the system can lose or gain stability. See Matsumoto and Szidarovszky (2015) and Gori et al. (2015) that adopt the methods for analyzing delay dynamics of Cournot duopoly. Also see Matsumoto et al. (2018), Gori et al (2017, 2018) and some papers in Matsumoto et al. (2016) for further applications of the methods to another economic models.

In this paper, we present different Cournot duopoly models with multiple delays as special cases of a general n-firm oligopoly. The first model includes both of the implementation and information delays, the second model possesses only the information delays and the third model is endowed with only the implementation delays. Applying the Lin-Wang method, we analytically and numerically investigate stability of these models and find that the delay models may explain various dynamics ranging from simple to complex behavior under Cournot competition.

This paper is organized as follows. Section 2 is divided into three subsections. In the first, we build a delay duopoly model based on HR's n-firm Cournot model and specify the parameter values and illustrate the stability switching curve under identical parameter condition. In the second, we focus on the special case where the firms have only information delays and confirm the corresponding HR result. In the third, we turn attention to a case where the firms have only implementation delays, the case which HR does not consider, to detect the properties of the information delay. In Section 3, we numerically examine how the stability properties change when certain nonlinearities are introduced into the adjustment process and the identical conditions are taken away. In the final section, concluding remarks and further research directions are given.

2 Delay Models

Constructing a Cournot profit maximizing model in which n firms have linear price and quadratic cost functions, HR derives a linear best reply function of firm i as

$$x_i^* = \alpha_i - \beta_i \sum_{j \neq i}^{n} x_j \text{ for } i,\ j = 1, 2, ...n \tag{1}$$

where α_i and β_i are positive constants and x_j is output of firm j. More precisely, in an n-firm linear Cournot oligopoly the price function is assumed to be

$$p\left(\sum_{i=1}^{n} x_i\right) = A - B\sum_{i=1}^{n} x_i$$

where A is the maximum (or reservation) price, $-B$ is the marginal price and $C_i x_i$ is the cost of firm i with zero fixed cost (which would have no effects on the optimal behavior of the firm). The profit of this firm is

$$\pi_i(x_i, x_{-i}) = x_i \left(A - Bx_i - B\sum_{j \neq i}^{n} x_j - C_i \right).$$

where $-i$ denotes the set of the competitors of firm i. With given outputs of the competitors the first order conditions of optimality imply that

$$\frac{\partial \pi_i}{\partial x_i} = A - 2Bx_i - B\sum_{j \neq i}^{n} x_j - C_i = 0$$

so the profit maximizing output of firm i is given as

$$x_i^* = \frac{A - C_i}{2B} - \frac{1}{2}\sum_{j \neq i}^{n} x_j$$

which is called the best reply of firm i and is identical to equation (1) with

$$\alpha_i = \frac{A - C_i}{2B} \text{ and } \beta_i = \frac{1}{2}.$$

If quadratic cost functions are assummed, then similarly to the previsous case, the best reply function still has the form (1) with slightly different parameters α_i and β_i.

In conventional Cournot oligopoly, it is usually assumed that the firms have full information on their own outputs but only imperfect information on their competitors' outputs. In reality, the firms also use delayed information on their own outputs since finding optimal decisions and their implementations need time. Therefore the best reply of each firm depends on past output of the firm and on past outputs of its competitors. Concerning the continuous-time adjustment of output, it is assumed that firm i adjusts its output at time t at a rate proportional to the difference between its best reply output and its actual output at some preceding times,

$$\frac{dx_i(t)}{dt} = k_i \left[x_i^*(t-\tau_{ib}) - x_i(t-\tau_{ia})\right] \text{ for } i = 1, 2, ..., n \tag{2}$$

where $(\tau_{ib}, \tau_{ia}) \geq 0$ denotes delays and $k_i > 0$ is the adjustment coefficient. If the best reply of a firm is higher than the observed output, then the firm wants to increase its output level at time t, if the best reply is smaller, then the firm wants to decrease its output level, and if they are equal, then the firm believes that it is on its optimal output level, so does not want to change its output level. If there are no delays $\tau_{ib} = \tau_{ia} = 0$ for all i, then (2) can be reduced to the traditional output adjustment system.

After determining Cournot-Nash equilibrium output x_i^e as the solution of equations

$$x_i^e + \beta_i \sum_{j \neq i}^{n} x_j^e = \alpha_i \text{ for } i, j = 1, 2, ..., n$$

HR provides a **sufficient condition** for stability of the equilibrium point,

$$\tau_i \leq \frac{1}{2k_i} \text{ for } i = 1, 2, ...n \tag{3}$$

under the parametric assumption

$$(n-1)\beta_i < 1.$$

It is very difficult to derive sufficient and necessary conditions for stability of the equilibrium point of equation (2) because of the variable number of firms and the $2n$ different delay parameters. Therefore in this study we focus on the two-firm case in which $-i$ contains only one firm which is denoted by j ($j \neq i$). In the special case of a linear duopoly with product differentiation (i.e., $B_i \neq \bar{B}_i$), the unit prices are as follows:

$$p_i(x_i, x_j) = A - 2B_i x_i - \bar{B}_i x_j \text{ for } i, j = 1, 2 \text{ and } j \neq i$$

so the profit of firm i becomes

$$\pi_i(x_i, x_j) = x_i \left(A - B_i x_i - \bar{B}_i x_j - C_i\right)$$

and the first order conditions imply that

$$A - 2B_i x_i - \bar{B}_i x_j - C_i = 0.$$

Therefore the best reply of firm i is as follows:

$$x_i^* = \frac{A - C_i}{2B_i} - \frac{\bar{B}_i}{2B_i} x_j$$

which is the duopoly version of equation (1) with

$$\alpha_i = \frac{A - C_i}{2B_i} \text{ and } \beta_i = \frac{\bar{B}_i}{2B_i}.$$

We will derive sufficient and necessary conditions for stability of the various versions of the delay HR model in the duopoly framework (i.e., $n = 2$) in which the Cournot-Nash equilibrium outputs are explicitly obtained,

$$x_1^e = \frac{\alpha_1 - \alpha_2\beta_1}{1 - \beta_1\beta_2} \text{ and } x_2^e = \frac{\alpha_2 - \alpha_1\beta_2}{1 - \beta_1\beta_2}.$$

To avoid negative output, we impose the following conditions on the parameters.

Assumption 1. $\beta_1\beta_2 < 1$ and $\beta_2 \leq \frac{\alpha_2}{\alpha_1} \leq \frac{1}{\beta_1}$.

To obtain the adjustment process of output, we substitute the delayed best replies $x_i^*(t-\tau_{ib}) = \alpha_i - \beta_i x_j(t-\tau_{ib})$ for $i = 1, 2$ into the delay differential equations (2) and consider its duopoly version in a more general way:

$$\begin{aligned} \frac{dx_1}{dt} &= k_1 \left[\alpha_1 - x_1(t-\tau_{1a}) - \beta_1 x_2(t-\tau_{1b})\right], \\ \frac{dx_2}{dt} &= k_2 \left[\alpha_2 - \beta_2 x_1(t-\tau_{2b}) - x_2(t-\tau_{2a})\right], \end{aligned} \tag{4}$$

where τ_{1a} and τ_{2a} are the delays in own outputs of the firms and τ_{1b} and τ_{2b} are the delays in the outputs of the competitors. In real economies such delays have to be taken into account. Delays in the own outputs of the firms are present since data collection and implementation need time. In the case of delays in the outputs of the competitors the delayed price information is an additional factor. From the price the firms are able to assess industry output and the competitor's output is obtained by the difference of the industry output and the firm's own output. The delays τ_{1a} and τ_{2a} on the firms own outputs are called the implementation delays and delays τ_{1b} and τ_{2b} on the best responses are called the information delays. It is, however, analytically intractable to analyze the asymptotic behavior of system (4) in general because of the presence of four distinct delays. Instead, three special cases will be examined and show how different delays affect the asymptotical behavior of the equilibrium.[1]

2.1 Model I (Duopoly version of the Howroyd-Russel model)

To have a duopoly version of the HR model, we assume that $\tau_{1a} = \tau_{1b} = \tau_1 \geq 0$ and $\tau_{2a} = \tau_{2b} = \tau_2 \geq 0$ leading to a model with only two delays. The stability properties of the equilibrium depend on the eigenvalues of the associated homogenous system,

$$\begin{aligned} \frac{dx_1}{dt} &= k_1 \left[-x_1(t-\tau_1) - \beta_1 x_2(t-\tau_1)\right], \\ \frac{dx_2}{dt} &= k_2 \left[-\beta_2 x_1(t-\tau_2) - x_2(t-\tau_2)\right]. \end{aligned} \tag{5}$$

With an exponential solution for the form

$$x_i = e^{\lambda t}\xi_i,$$

the characteristic equation of (5) is derived as

$$\det \begin{pmatrix} \lambda + k_1 e^{-\lambda\tau_1} & k_1\beta_1 e^{-\lambda\tau_1} \\ k_2\beta_2 e^{-\lambda\tau_2} & \lambda + k_2 e^{-\lambda\tau_2} \end{pmatrix} = 0$$

[1] HR considers the case where the delay in the own output of firm k is the same as the delays in its competitors, $\tau_{kj} = \tau_k$ for $j = 1, 2, ..., n$. We adopt the same assumption in the following.

or

$$P_0(\lambda) + P_1(\lambda)e^{-\lambda\tau_1} + P_2(\lambda)e^{-\lambda\tau_2} + P_3(\lambda)e^{-\lambda(\tau_1+\tau_2)} = 0 \tag{6}$$

where

$$P_0(\lambda) = \lambda^2,\ P_1(\lambda) = k_1\lambda,\ P_2(\lambda) = k_2\lambda,\ P_3(\lambda) = k_1k_2(1-\beta_1\beta_2).$$

The dynamic system (5) describes the case where the firm believes that the delay of the competitor is the same as its own. Notice that even if the firms can correctly predict the delays of their competitors, the dynamic results to be obtained are the same. This is because the corresponding dynamic system is constructed by interchanging the delays in the off-diagonal outputs of system (5) and thus the characteristic equation of the new system is identical with equation (6) implying that the resultant (local) dynamics is the same. Also notice that this similarity holds only in the duopoly framework.

If the characteristic equation (6) has roots only with the negative real parts, then the zero solution of delay system (5) is locally asymptotically stable. Thus our problem is to determine parametric conditions under which all roots of the characteristic equation lie in the left half of the complex plane. As a benchmark, suppose that $\tau_1 = \tau_2 = 0$. Then (6) becomes

$$\lambda^2 + (k_1 + k_2)\,\lambda + k_1k_2(1-\beta_1\beta_2) = 0$$

where the two roots of this equation are real and negative if $\beta_1\beta_2 < 1$. Hence Assumption 1 guarantees stability of the stationary point of the duopoly model with no-delay. We now suppose that $\tau_1 \geq 0$ and $\tau_2 \geq 0$ but not $\tau_1 = \tau_2 = 0$. It is assumed that (τ_1, τ_2) varies continuously in $R^2_+ = \{(\tau_1, \tau_2) \mid \tau_1 \geq 0 \text{ and } \tau_2 \geq 0)\}$. Since $\lambda = 0$ is not a root of (6), the number of eigenvalues having a positive real part can change only if an eigenvalue appears on or crosses the imaginary axis. Therefore in order to study stability, we need to find all pure complex roots of equation (6). We thus look for a pair of delays for which (6) has purely imaginary roots. Since roots of real function always come in conjugate pairs, it can be assumed, without loss of generality, that $\lambda = i\omega$ with $\omega > 0$. Substituting it into (6) presents the form

$$P_0(i\omega) + P_1(i\omega)e^{-i\omega\tau_1} + P_2(i\omega)e^{-i\omega\tau_2} + P_3(i\omega)e^{-i\omega(\tau_1+\tau_2)} = 0 \tag{7}$$

with

$$P_0(i\omega) = -\omega^2,\ P_1(i\omega) = ik_1\omega,\ P_2(i\omega) = ik_2\omega,\ P_3(i\omega) = k_1k_2(1-\beta_1\beta_2). \tag{8}$$

Applying the method developed by Lin and Wang (2012), we derive the set of (τ_1, τ_2) for which the delay dynamic system (5) loses stability. Equation (7) can be rewritten as

$$\left(P_0 + P_1e^{-i\omega\tau_1}\right) + \left(P_2 + P_3e^{-i\omega\tau_1}\right)e^{-i\omega\tau_2} = 0 \tag{9}$$

where the arguments of $P_0,\ P_1,\ P_2$ and P_3 are omitted for the sake of simplicity. Since $\left|e^{-i\omega\tau_2}\right| = 1$, equation (9) has solution for τ_1 if and only if

$$\left|P_0 + P_1e^{-i\omega\tau_1}\right| = \left|P_2 + P_3e^{-i\omega\tau_1}\right|$$

or equivalently,

$$\left(P_0 + P_1e^{-i\omega\tau_1}\right)\left(\bar{P}_0 + \bar{P}_1e^{i\omega\tau_1}\right) = \left(P_2 + P_3e^{-i\omega\tau_1}\right)\left(\bar{P}_2 + \bar{P}_3e^{i\omega\tau_1}\right),$$

where over-bar indicates complex conjugate. After some algebra, the last equation has the form

$$|P_0|^2 + |P_1|^2 - |P_2|^2 - |P_3|^2 = 2A_1(\omega)\cos\omega\tau_1 - 2B_1(\omega)\sin\omega\tau_1 \tag{10}$$

with

$$A_1(\omega) = \mathrm{Re}\left(P_2\bar{P}_3 - P_0\bar{P}_1\right) \text{ and } B_1(\omega) = \mathrm{Im}\left(P_2\bar{P}_3 - P_0\bar{P}_1\right).$$

The left hand side of equation (10) depends only on ω and the right hand side is a simple trigonometric equation for τ_1 with any fixed value of ω. Denoting the left hand side by $f(\omega)$, we first check the existence of solutions for equation (10).

Using (8), we can confirm that

$$P_2\bar{P}_3 - P_0\bar{P}_1 = ik_1\omega\left[k_2^2\left(1-\beta_1\beta_2\right) - \omega^2\right]$$

implying that

$$A_1(\omega) = 0 \text{ and } B_1(\omega) = k_1\omega\left[k_2^2\left(1-\beta_1\beta_2\right) - \omega^2\right].$$

We examine the case of $B_1(\omega) = 0$ and then the case of $B_1(\omega) \neq 0$ in the following.

Case I. $A_1(\omega) = B_1(\omega) = 0$

Let ω_0 be the positive solution of $B_1(\omega) = 0$,

$$\omega_0 = k_2\sqrt{1-\beta_1\beta_2} > 0.$$

Substituting $P_j(i\omega)$ for $j = 0, 1, 2, 3$ defined in (8) into $f(\omega)$ gives

$$f(\omega) = \omega^4 + \left(k_1^2 - k_2^2\right)\omega^2 - \left(k_1k_2\right)^2\left(1-\beta_1\beta_2\right)^2.$$

Then solving $f(\omega) = 0$ for ω^2 yields a positive solution

$$\omega_+^2 = \frac{-\left(k_1^2-k_2^2\right) + \sqrt{\left(k_1^2-k_2^2\right)^2 + 4\left(k_1k_2\right)^2\left(1-\beta_1\beta_2\right)^2}}{2} > 0$$

that is reduced to ω_0^2 if $k_1 = k_2$ and not equal to it if $k_1 \neq k_2$. We then have two possibilities. First, if $k_1 \neq k_2$, then $f(\omega) \neq 0$ for $\omega = \omega_0$. Thus there is no solution for τ_1 since equation (10) is contradicted. On the other hand, if $k_1 = k_2$, then $f(\omega) = 0$ for $\omega = \omega_0$. Thus $\tau_1 > 0$ is arbitrary, and the corresponding values of τ_2 can be obtained from equation (9) as

$$e^{-i\omega\tau_2} = -\frac{P_0(i\omega) + P_1(i\omega)e^{-i\omega\tau_1}}{P_2(i\omega) + P_3(i\omega)e^{-i\omega\tau_1}} \tag{11}$$

where the absolute value of the right hand side is unity for all values of τ_1. Therefore there are infinitely many solutions of τ_2 because of periodicity of trigonometric functions. A locus of τ_1 and τ_2 satisfying (11) is called a *crossing curve* on which roots of (7) cross the imaginary axis when τ_2 changes and τ_1 is fixed (or alternatively τ_1 changes and τ_2 is fixed). Since the zero solution of (5) is locally asymptotically stable with no delays and its stability depends on the lengths of the positive delays, there may be the curve on which the stability of the zero solution changes. We call such a curve a *stability switching curve*. The result obtained is summarized as follows:

Theorem 1 *If the adjustment coefficients of the two firms are identical (i.e., $k_1 = k_2$), then the crossing curve in Case I is described by $(\tau_1, \tau_2^\ell(\tau_1))$ where*

$$\tau_2^\ell(\tau_1) = \frac{1}{\omega_0}\left\{\arg\left[-\frac{P_2(i\omega_0) + P_3(i\omega_0)e^{-i\omega_0\tau_1}}{P_0(i\omega_0) + P_1(i\omega_0)e^{-i\omega_0\tau_1}}\right] + 2\ell\pi\right\} \text{ for } \ell = 0,\ \pm1,\ \pm2, ... \tag{12}$$

Case II. $[A_1(\omega)]^2 + [B_1(\omega)]^2 > 0$

We have already known that $A_1(\omega) = 0$ for any $\omega \geq 0$ and $B_1(\omega) \neq 0$ for $\omega \neq \omega_0$. There exists $\varphi_1(\omega)$ such that

$$\varphi_1(\omega) = \arg\left[P_2\bar{P}_3 - P_0\bar{P}_1\right] = \begin{cases} \dfrac{\pi}{2} & \text{if } B_1(\omega) > 0 \text{ or } \omega < \omega_0, \\ \dfrac{3\pi}{2} & \text{if } B_1(\omega) < 0 \text{ or } \omega > \omega_0, \end{cases}$$

implying that

$$\sin[\varphi_1(\omega)] = \frac{B_1(\omega)}{\sqrt{[B_1(\omega)]^2}} \text{ and } \cos[\varphi_1(\omega)] = \frac{A_1(\omega)}{\sqrt{[B_1(\omega)]^2}} = 0.$$

Using these relations, Equation (10) is reduced to

$$|P_0|^2 + |P_1|^2 - |P_2|^2 - |P_3|^2 = 2\sqrt{[B_1(\omega)]^2}\cos(\varphi_1(\omega) + \omega\tau_1) \tag{13}$$

that can be rewritten as

$$\frac{|P_0|^2 + |P_1|^2 - |P_2|^2 - |P_3|^2}{2\sqrt{[B_1(\omega)]^2}} = \cos[\varphi_1(\omega) + \omega\tau_1].$$

A sufficient and necessary conditions for the existence of $\tau_1 \geq 0$ satisfying the above equation is

$$\left||P_0|^2 + |P_1|^2 - |P_2|^2 - |P_3|^2\right| \leq 2\sqrt{[B_1(\omega)]^2}$$

or

$$F(\omega) = \left[|P_0|^2 + |P_1|^2 - |P_2|^2 - |P_3|^2\right]^2 - 4[B_1(\omega)]^2 \leq 0.$$

With the notation of $x = \omega^2$, the right hand side of $F(\omega)$ is reduced to the following form

$$g(x) = x^4 + a_3x^3 + a_2x^2 + a_1x + a_0$$

where the coefficients are defined as

$$\begin{aligned} a_3 &= -2(k_1^2 + k_2^2), \\ a_2 &= (k_1^2 - k_2^2)^2 + 2(k_1k_2)^2(3 + \beta_1\beta_2)(1 - \beta_1\beta_2), \\ a_1 &= -2(k_1^2 + k_2^2)[k_1k_2(1 - \beta_1\beta_2)]^2, \\ a_0 &= [k_1k_2(1 - \beta_1\beta_2)]^4. \end{aligned}$$

Solving $g(x) = 0$ yields four real solutions,

$$\begin{aligned} x_1 &= \frac{1}{2}\left[k_1^2 + k_2^2 - 2k_1k_2\beta_1\beta_2 - (k_1 - k_2)\sqrt{d_1}\right], \\ x_2 &= \frac{1}{2}\left[k_1^2 + k_2^2 - 2k_1k_2\beta_1\beta_2 + (k_1 - k_2)\sqrt{d_1}\right], \\ x_3 &= \frac{1}{2}\left[k_1^2 + k_2^2 + 2k_1k_2\beta_1\beta_2 - (k_1 + k_2)\sqrt{d_2}\right], \\ x_4 &= \frac{1}{2}\left[k_1^2 + k_2^2 + 2k_1k_2\beta_1\beta_2 + (k_1 + k_2)\sqrt{d_2}\right], \end{aligned}$$

where both discriminants are positive,

$$d_1 = (k_1 + k_2)^2 - 4k_1k_2\beta_1\beta_2 > 0$$

and

$$d_2 = (k_1 - k_2)^2 + 4k_1k_2\beta_1\beta_2 > 0.$$

Positive solutions of $x_i = \omega^2$ are denoted by ω_i where

$$\omega_3 < \omega_4 \text{ and } \omega_1 \lessgtr \omega_2 \text{ according to } k_1 \lessgtr k_2.$$

The interval $[\omega_3, \omega_i] \cup [\omega_j, \omega_4]$ is denoted by Ω in which $F(\omega) \leq 0$ and $\omega_i = \omega_1$ and $\omega_j = \omega_2$ if $k_1 > k_2$ and ω_i is interchanged with ω_j if the inequality is reversed.

Let us define $\psi_1(\omega)$ by

$$|P_0|^2 + |P_1|^2 - |P_2|^2 - |P_3|^2 = 2\sqrt{B_1(\omega)^2}\cos\left[\psi_1(\omega)\right]. \tag{14}$$

So

$$\psi_1(\omega) = \cos^{-1}\left[\frac{|P_0|^2 + |P_1|^2 - |P_2|^2 - |P_3|^2}{2\sqrt{B_1(\omega)^2}}\right].$$

Comparing the right hand side of (13) with that of (14) yields

$$\tau_{1,n}^{\pm}(\omega) = \frac{1}{\omega}\left[\pm\psi_1(\omega) - \varphi_1(\omega) + 2n\pi\right]. \tag{15}$$

Returning to (7), we can see that it can be alternatively put as

$$\left(P_0 + P_2e^{-i\omega\tau_2}\right) + \left(P_1 + P_3e^{-i\omega\tau_2}\right)e^{-i\omega\tau_1} = 0.$$

In the similar way as shown for τ_1, we can find the critical values of τ_2 as

$$\tau_{2,m}^{\pm}(\omega) = \frac{1}{\omega}\left[\pm\psi_2(\omega) - \varphi_2(\omega) + 2m\pi\right] \tag{16}$$

where

$$\begin{aligned} A_2(\omega) &= \mathrm{Re}\left[P_1\bar{P}_3 - P_0\bar{P}_2\right] = 0, \\ B_2(\omega) &= \mathrm{Im}\left[P_1\bar{P}_3 - P_0\bar{P}_2\right] = k_2\omega\left[k_1^2(1 - \beta_1\beta_2) - \omega^2\right], \end{aligned}$$

$$\psi_2(\omega) = \cos^{-1}\left[\frac{|P_0|^2 - |P_1|^2 + |P_2|^2 - |P_3|^2}{2\sqrt{B_2(\omega)^2}}\right]$$

and

$$\varphi_2(\omega) = \arg\left[P_1\bar{P}_3 - P_0\bar{P}_2\right] = \begin{cases} \dfrac{\pi}{2} & \text{if } B_2(\omega) > 0, \\ \dfrac{3\pi}{2} & \text{if } B_2(\omega) < 0. \end{cases}$$

To define $\psi_2(\omega)$, we need a condition similar to $F(\omega) \leq 0$, that is,

$$G(\omega) = \left(|P_0|^2 - |P_1|^2 + |P_2|^2 - |P_3|^2\right)^2 - 4\left[B_2(\omega)\right]^2 \leq 0.$$

Since it can be shown that $F(\omega) = G(\omega)$, solutions of $F(\omega) = 0$ solve $G(\omega) = 0$. The results obtained so far are summarized as follows:

Theorem 2 *From* (15) *and* (16)*, the following pair of delays*

$$\left\{(\tau_{1,m}^{\pm}(\omega),\ \tau_{2,n}^{\mp}(\omega)) \mid \omega \in \Omega\right\}$$

is the set of all crossing curves on the (τ_1, τ_2) *plane for equations* (5)*.*

We will now turn to the special case of **identical adjustment coefficients** by considering the above-mentioned two cases further by performing numerical simulations to visualize the theoretical results obtained in Theorems 1 and 2. For this purpose, we make the following assumption of identical adjustment coefficients under which we examine Case I and then Case II.

Assumption 2. $k_1 = k_2 = k$

In Case I, an explicit form of τ_2^{ℓ} with $\ell = 0$ described by (12) is derived as follows. Applying Euler's formula to the left hand side of (11) and substituting P_i defined in (8) into the right hand side lead to

$$\cos\omega\tau_2 - i\sin\omega\tau_2 \quad = \frac{\left(\omega^2 - k\omega\sin\omega\tau_1\right) - ik\omega\cos\omega\tau_1}{k^2(1-\beta_1\beta_2)\cos\omega\tau_1 + i\left(k\omega - k^2(1-\beta_1\beta_2)\sin\omega\tau_1\right)}. \tag{17}$$

Multiplying by conjugate of denominator, the new denominator becomes

$$D_1 = k^2\left[k^2(1-\beta_1\beta_2)^2 - 2k\omega(1-\beta_1\beta_2)\sin\omega\tau_1 + \omega^2\right].$$

The new numerator is denoted as $N_1 + iM_1$ with

$$N_1 = -(k\omega)^2\beta_1\beta_2\cos\omega\tau_1$$

and

$$M_1 = -k\omega\left[k^2(1-\beta_1\beta_2) + \omega^2\right] + (k\omega)^2(2-\beta_1\beta_2)\sin\omega\tau_1.$$

Comparing the left hand side of (17) with $N_1/D_1 + iM_1/D_1$ yields

$$\cos\omega\tau_2 = \frac{N_1}{D_1} \text{ and } \sin\omega\tau_2 = -\frac{M_1}{D_1} \tag{18}$$

where the graphs of N_1/D_1 and $-M_1/D_1$ as functions of τ_1 are illustrated in Figure 1 for $\tau_1 \in [0, 2\pi]$ under the following benchmark parameter values $k = 1$, $\alpha_1 = \alpha_2 = 9$ and $\beta_1 = \beta_2 = 1/2$. These values are repeatedly used in the following numerical calculations. Each of the red N_1/D_1 curve and the blue $-M_1/D_1$ curve intersects the horizontal axis twice at the following points,

$$\tau_1^B \simeq 1.81,\ \tau_1^D \simeq 5.44 \text{ and } \tau_1^A \simeq 1.65,\ \tau_1^C \simeq 1.98.$$

We will refer to the dotted red curve later.

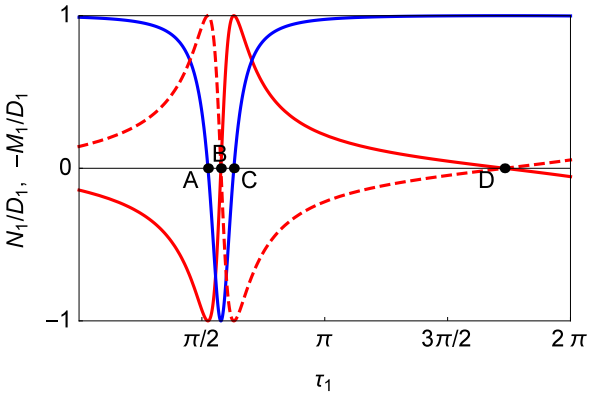

Figure 1. Graphs of N_1/D_1 (red) and $-M_1/D_1$ (blue)

It is observed that $\cos\omega\tau_2 < 0$ and $\sin\omega\tau_2 > 0$ for $\tau_1 \in (0, \tau_1^A)$. Hence solving $\cos\omega\tau_2 = N_1/D_1$ and $\sin\omega\tau_2 = -M_1/D_1$ for τ_2 yields

$$\tau_2^c(\tau_1) = \frac{1}{\omega}\cos^{-1}\left(\frac{N_1}{D_1}\right) \text{ and } \tau_2^s(\tau_1) = \frac{1}{\omega}\left[\pi - \sin^{-1}\left(-\frac{M_1}{D_1}\right)\right] \tag{19}$$

where the superscripts c and s stand for cos and sin, respectively. In the same way, $\cos\omega\tau_2 < 0$ and $\sin\omega\tau_2 < 0$ for $\tau_1 \in (\tau_1^A, \tau_1^B)$ that present

$$\tau_2^c(\tau_1) = \frac{1}{\omega}\left[2\pi - \cos^{-1}\left(\frac{N_1}{D_1}\right)\right] \text{ and } \tau_2^s(\tau_1) = \frac{1}{\omega}\left[\pi - \sin^{-1}\left(-\frac{M_1}{D_1}\right)\right]. \tag{20}$$

For $\tau_1 \in (\tau_1^B, \tau_1^C)$, $\cos\omega\tau_2 > 0$ and $\sin\omega\tau_2 < 0$ gives

$$\tau_2^c(\tau_1) = \frac{1}{\omega}\left[2\pi - \cos^{-1}\left(\frac{N_1}{D_1}\right)\right] \text{ and } \tau_2^s(\tau_1) = \frac{1}{\omega}\left[2\pi + \sin^{-1}\left(-\frac{M_1}{D_1}\right)\right]. \tag{21}$$

Finally for $\tau_1 \in (\tau_1^C, \tau_1^D) \cup [\tau_1^D, 2\pi]$, $\cos\omega\tau_2 > 0$ and $\sin\omega\tau_2 > 0$ generate

$$\tau_2^c(\tau_1) = \frac{1}{\omega}\cos^{-1}\left(\frac{N_1}{D_1}\right) \text{ and } \tau_2^s(\tau_1) = \frac{1}{\omega}\sin^{-1}\left(-\frac{M_1}{D_1}\right). \tag{22}$$

Since $\tau_2^s(\tau_1) = \tau_2^c(\tau_1)$ holds for any $\tau_1 \in [0, 2\pi]$, the solution can be denoted by $\tau_2(\tau_1)$.

The locus of $(\tau_1, \tau_2(\tau_1))$ for $\tau_1 \in [0, 2\pi]$ constructs the stability switching curve in Case I that is illustrated by two black curves in Figure 2. More precisely, the upper convex-shaped curve consists of three segments, each of which is described by (19), (20) and (21) whereas the lower concave-shaped curve is described only by (22).[2] It is numerically confirmed that the upper curve passes through point $\left(2\pi/3\sqrt{3}, 4\pi/3\sqrt{3}\right)$ at which the blue curve ends and the orange curve starts and that the lower curve passes through point $\left(4\pi/3\sqrt{3}, 2\pi/3\sqrt{3}\right)$ at which the green curve starts and the red curve ends.

In Case II with Assumption 2, solving $F(\omega) = 0$ yields simplified solutions,

$$\omega_1 = \omega_2 = k\sqrt{1-\beta_1\beta_2},\ \omega_3 = k(1-\sqrt{\beta_1\beta_2}) \text{ and } \omega_4 = k(1+\sqrt{\beta_1\beta_2}),$$

implying that

$$\Omega = [\omega_3, \omega_1] \cup [\omega_2, \omega_4].$$

[2] However, only some parts of the curves are illustrated for graphical simplicity.

Since $\omega_0 = \omega_i$ for $i = 1, 2$,

$$B_i(\omega) > 0 \text{ for } \omega \in [\omega_3, \omega_1) \text{ implying } \varphi_i(\omega) = \pi/2,$$
$$B_i(\omega) < 0 \text{ for } \omega \in (\omega_2, \omega_4] \text{ implying } \varphi_i(\omega) = 3\pi/2.$$

In Figure 2, the blue and red curves are described by the pairs of

$$\left(\tau^+_{1,0}(\omega),\ \tau^-_{2,1}(\omega)\right) \text{ and } \left(\tau^-_{1,1}(\omega),\ \tau^+_{1,0}(\omega)\right) \text{ for } \omega \in [\omega_3, \omega_1]$$

starting at point (π, π) for $\omega = \omega_3$. On the other hand, the green and orange curves are described by the pairs of

$$\left(\tau^+_{1,1}(\omega),\ \tau^-_{2,1}(\omega)\right) \text{ and } \left(\tau^-_{1,1}(\omega),\ \tau^+_{2,1}(\omega)\right) \text{ for } \omega \in [\omega_2, \omega_4]$$

ending at point $(\pi/3, \pi/3)$ for $\omega = \omega_4$. Hence the stationary point is stable in the lower-left region surrounded by the two black, orange and green curves. The hatched square is the region satisfying the HR conditions, (3). Notice that the square is inside the stable region we have just obtained. This is because HR derives one sufficient condition whereas we derive the sufficient and necessary condition. We will refer to the vertical dotted lines at $\tau_1 = \pi/3$ and $\tau_1 = 4\pi/3\sqrt{3}$ and points a, b, c later when we will perform numerical simulations.

Theorem 3 *The equilibrium point of dynamic system* (5) *is locally asymptotically stable for* (τ_1, τ_2) *in the region bounded by the stability switching curve that consists of the black, orange and green curves in the non-negative quadrant of* (τ_1, τ_2).

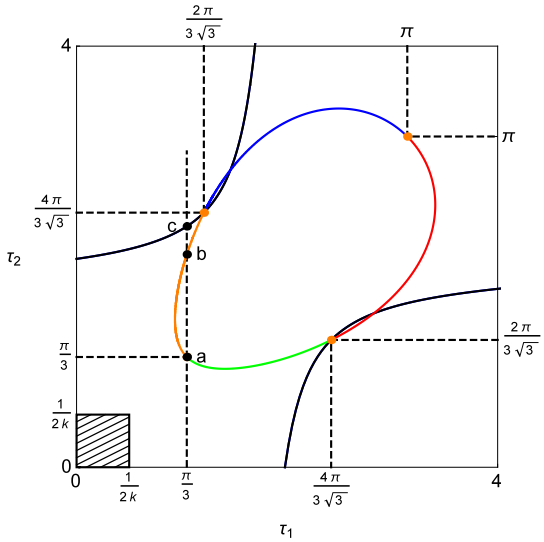

Figure 2. Division of the (τ_1, τ_2) plane

2.2 Delay Duopoly Model II

In the previous section the combined effect of the identical information and implementation delays was examined without discovering which delay is more responsible for the complex dynamics being observed. One simple way is to consider models where only one type of delays is present and examine the long-term behavior of the simplified models. HR also examines the case where

each firm has delayed information on its competitor's outputs but instantaneous knowledge of its own output. In a perfect world, the best reply of firm i depends on the current level of output of the competitor j, $x_j(t)$ whereas, in the real world, this information may not be available and firm i takes the delayed output $x_j(t-\tau_i)$ as a proxy for $x_j(t)$.[3] Thus, the homogenous system of the corresponding delay differential equations with $n=2$ is

$$\begin{aligned} \frac{dx_1}{dt} &= k_1\left[-x_1(t)-\beta_1 x_2(t-\tau_1)\right], \\ \frac{dx_2}{dt} &= k_2\left[-\beta_2 x_1(t-\tau_2)-x_2(t)\right], \end{aligned} \tag{23}$$

where only the non-diagonal variables are delayed. This is a special case of equation (4) with $\tau_{1a}=\tau_{2a}=0,\ \tau_{1b}=\tau_1$ and $\tau_{2b}=\tau_2$. The characteristic equation is

$$\det\begin{pmatrix} \lambda+k_1 & k_1\beta_1 e^{-\lambda\tau_1} \\ k_2\beta_2 e^{-\lambda\tau_2} & \lambda+k_2 \end{pmatrix}=0$$

or

$$\lambda^2+k_1k_2+(k_1+k_2)\lambda-k_1k_2\beta_1\beta_2e^{-\lambda\tau}=0 \tag{24}$$

where $\tau=\tau_1+\tau_2>0$. Since τ_1 can be different from τ_2, firms have heterogenous abilities to gather information about competitor's output. However this heterogeneity does not affect local stability. As seen in equation (24), only the value of the sum of these delays can affect local stability of the equilibrium. Dynamic system (23) with two different delays, τ_1 and τ_2, is essentially the same as a dynamic system with a single delay τ. Suppose $\lambda=i\omega$ with $\omega>0$ is a root of (24) for some τ and substitute it into (24) that can be separated to the real and imaginary parts,

$$-\omega^2+k_1k_2-k_1k_2\beta_1\beta_2\cos\omega\tau=0,$$

$$(k_1+k_2)\omega+k_1k_2\beta_1\beta_2\sin\omega\tau=0.$$

Moving the non-trigonometric terms to the right hand side and adding the squares of the two equations yield a biquadratic equation of ω

$$\omega^4+\left(k_1^2+k_2^2\right)\omega^2+\left(k_1k_2\right)^2\left[1-(\beta_1\beta_2)^2\right]=0$$

where the last term is positive due to Assumption 2. Positive coefficients of this equation imply that no real solutions exist, therefore there are no pure imaginary roots for equation (24).

In other words, there are no roots of (24) that cross the imaginary axis when τ increases. Therefore no stability switch can occur, no matter how the delays are chosen. Such delays are called *harmless*. This is the same as the result shown by HR in a different way and can be summarized as follow.

Theorem 4 *The equilibrium point of dynamic system of* (23) *is locally asymptotically stable regardless of the values of* τ_1 *and* τ_2.

[3] This justification for Model II is suggested by a referee.

2.3 Delay Duopoly Model III

Model I indicates that the coexistence of the implementation and information delays can destabilize the equilibrium. On the other hand, Model II suggests that the information delay alone does not affect stability of the equilibrium. As natural consequence, it is worth while looking more carefully into the role of the implementation delays. For this purpose we consider the case where only implementation delay is present. We note that it is hard to justify its economic application however it might explain long-term dynamics if both types of delays are present. Therefore, we consider the case in which each firm has delayed knowledge of its own output but instantaneous knowledge of its competitors' outputs. In this way, we can shed light on the actual role of the implementation delay where the homogeneous dynamic system is constructed in the following way,

$$\begin{aligned} \frac{dx_1}{dt} &= k_1 \left[-x_1(t-\tau_1) - \beta_1 x_2(t) \right], \\ \frac{dx_2}{dt} &= k_2 \left[-\beta_2 x_1(t) - x_2(t-\tau_2) \right] \end{aligned} \tag{25}$$

where the diagonal variables are delayed. This case also has mathematical interest to see how different delay structure changes the dynamic properties of the equilibrium. With the same procedure above, we obtain the characteristic equation,

$$\det \begin{pmatrix} \lambda + k_1 e^{-\lambda\tau_1} & k_1\beta_1 \\ k_2\beta_2 & \lambda + k_2 e^{-\lambda\tau_2} \end{pmatrix} = 0$$

that is equivalent to the equation

$$P_0(\lambda) + P_1(\lambda)e^{-\lambda\tau_1} + P_2(\lambda)e^{-\lambda\tau_2} + P_3(\lambda)e^{-\lambda(\tau_1+\tau_2)} = 0 \tag{26}$$

where

$$P_0(\lambda) = \lambda^2 - k_1k_2\beta_1\beta_2,\ P_1(\lambda) = k_1\lambda,\ P_2(\lambda) = k_2\lambda,\ P_3(\lambda) = k_1k_2.$$

Although each firm has a delay only in its own output, the characteristic equation (26) has the similar form to (7) in which each firm has not only the implementation delay on its own output but also the information delay on its competitor's output. Supposing $\lambda = i\omega$ with $\omega > 0$ and then following the same procedure as in Section 2, we have

$$|P_0(i\omega)|^2 + |P_1(i\omega)|^2 - |P_2(i\omega)|^2 - |P_3(i\omega)|^2 = 2A_1(\omega)\cos\omega\tau_1 - 2B_1(\omega)\sin\omega\tau_1$$

with

$$\begin{aligned} A_1(\omega) &= \mathrm{Re}\left[P_2(i\omega)\bar{P}_3(i\omega) - P_0(i\omega)\bar{P}_1(i\omega)\right] = 0, \\ B_1(\omega) &= \mathrm{Im}\left[P_2(i\omega)\bar{P}_3(i\omega) - P_0(i\omega)\bar{P}_1(i\omega)\right] = k_1\omega\left(k_2^2 - k_1k_2\beta_1\beta_2 - \omega^2\right). \end{aligned}$$

As before, we first consider the case of $A_1(\omega) = B_1(\omega) = 0$. It can be confirmed that $A_1(\omega) = 0$ always and $B_1(\omega) = 0$ holds for $\omega = \omega_0$ where

$$\omega_0^2 = k_2^2 - k_1k_2\beta_1\beta_2.$$

On the other hand, $|P_0(i\omega)|^2 + |P_1(i\omega)|^2 - |P_2(i\omega)|^2 - |P_3(i\omega)|^2 = 0$ for $\omega = \omega_+$ where

$$\omega_+^2 = \frac{\left(k_2^2 - 2k_1k_2\beta_1\beta_2 - k_1^2\right) + \sqrt{\left(k_2^2 - 2k_1k_2\beta_1\beta_2 - k_1^2\right)^2 + 4\left(k_1k_2\right)^2\left[1 - (\beta_1\beta_2)^2\right]}}{2}.$$

If $k_1 = k_2 = k$, then ω_0 and ω_+ are the same

$$\omega_0 = \omega_+ = k\sqrt{1-\beta_1\beta_2}$$

and this equality does not hold if $k_1 \neq k_2$. Hence, under the identical coefficient assumption, the stability switching curve is obtained as

$$e^{-i\omega_0\tau_2} = -\frac{P_0(i\omega_0) + P_1(i\omega_0)e^{-i\omega_0\tau_1}}{P_2(i\omega_0) + P_3(i\omega_0)e^{-i\omega_0\tau_1}}. \tag{27}$$

As in the same analysis of Section 2.1, equation (27) can be rewritten as

$$\cos\omega_0\tau_2 - i\sin\omega_0\tau_2 = \frac{\left(\omega_0^2 + k^2\beta_1\beta_2 - k\omega_0\sin\omega_0\tau_1\right) - ik\omega_0\cos\omega_0\tau_1}{k^2\cos\omega_0\tau_1 + i\left(k\omega_0 - k^2\sin\omega_0\tau_1\right)}. \tag{28}$$

Multiplying conjugate of denominator to the denominator and numerator of the right hand side of (28) leads to the new denominator

$$D_3 = k^2\left(k^2 - 2k\omega_0\sin\omega_0\tau_1 + \omega_0^2\right) \tag{29}$$

and the new numerator

$$N_3 + iM_3$$

where

$$N_3 = k^4\beta_1\beta_2\cos\omega_0\tau_1$$

and

$$M_3 = -k\omega_0\left(k^2 + \omega_0^2 + k^2\beta_1\beta_2\right) + k^2\left(2\omega_0^2 + k^2\beta_1\beta_2\right)\sin\omega_0\tau_1.$$

Hence from the left hand side of (28) we have

$$\cos\omega_0\tau_2 = \frac{N_3}{D_3} \text{ and } \sin\omega_0\tau_2 = -\frac{M_3}{D_3} \tag{30}$$

where

$$\frac{N_3}{D_3} = \frac{k^2\beta_1\beta_2\cos\omega_0\tau_1}{k^2 - 2k\omega_0\sin\omega_0\tau_1 + \omega_0^2} = -\frac{N_1}{D_1}$$

and

$$\frac{M_3}{D_3} = \frac{-2k\omega_0 + (k^2+\omega_0^2)\sin\omega_0\tau_1}{k^2 - 2k\omega_0\sin\omega_0\tau_1 + \omega_0^2} = -\frac{M_1}{D_1}.$$

Comparing (30) with (18) reveals that in Figure 1, the M_3/D_3 curve is identical with the M_1/D_1 blue curve whereas the N_3/D_3 curve corresponds to the dotted red curve, that is, a horizontal-line mirror image of the N_1/D_1 red curve.

We now turn attention to the case of $[B_1(\omega)]^2 > 0$. As is shown above, we should have

$$F(\omega) = \left[|P_0|^2 + |P_1|^2 - |P_2|^2 - |P_3|^2\right]^2 - 4\left[B_1(\omega)\right]^2 \leq 0$$

where $F(\omega)$ can be factored as

$$F(\omega) = F_a(\omega)\cdot F_b(\omega)\cdot F_c(\omega)\cdot F_d(\omega)$$

with

$$F_a(\omega) = \omega^2 + (k_1 + k_2)\omega + k_1 k_2 \left(1 + \beta_1 \beta_2\right),$$
$$F_b(\omega) = \omega^2 - (k_1 + k_2)\omega + k_1 k_2 \left(1 + \beta_1 \beta_2\right),$$
$$F_c(\omega) = \omega^2 + (k_1 - k_2)\omega - k_1 k_2 \left(1 - \beta_1 \beta_2\right),$$
$$F_d(\omega) = \omega^2 - (k_1 - k_2)\omega - k_1 k_2 \left(1 - \beta_1 \beta_2\right).$$

Solving each $F_i(\omega) = 0$ for $i = a, b, c, d$ yields two solutions and totally eight solutions are obtained,

$$\omega_{\pm}^a = \frac{k_1 + k_2 \pm \sqrt{(k_1 + k_2)^2 - 4k_1 k_2 \left(1 + \beta_1 \beta_2\right)}}{2} = k\left(1 \pm i\sqrt{\beta_1 \beta_2}\right),$$
$$\omega_{\pm}^b = \frac{-(k_1 + k_2) \pm \sqrt{(k_1 + k_2)^2 - 4k_1 k_2 \left(1 + \beta_1 \beta_2\right)}}{2} = k\left(-1 \pm i\sqrt{\beta_1 \beta_2}\right),$$
$$\omega_{\pm}^c = \frac{k_1 - k_2 \pm \sqrt{(k_1 - k_2)^2 + 4k_1 k_2 \left(1 - \beta_1 \beta_2\right)}}{2} = \pm k\sqrt{1 - \beta_1 \beta_2},$$
$$\omega_{\pm}^d = \frac{-(k_1 - k_2) \pm \sqrt{(k_2 - k_1)^2 + 4k_1 k_2 \left(1 - \beta_1 \beta_2\right)}}{2} = \pm k\sqrt{1 - \beta_1 \beta_2}.$$

Notice that the right most forms are obtained under the identical coefficient assumption. We see $F(\omega) > 0$ for $\omega \neq \omega_0$, implying no occurrence of the stability switch in the case of $[B_1(\omega)]^2 > 0$.

Returning to Figure 1 and (30), the stability switching curve with $B_1(\omega) = 0$ illustrated in Figure 3(A) is constructed as follows. Since $\cos\omega\tau_1 > 0$ and $\sin\omega\tau_1 > 0$ for $\tau_1 \in (0, \tau_1^A)$, we have

$$\tau_2^A(\tau_1) = \frac{1}{\omega_0}\cos^{-1}\left(\frac{N_3}{D_3}\right) \tag{31}$$

that describes the concave-shaped negative slope red curve in the lower-left corner. Since the stationary state is stable below the curve and unstable above, this is the stability switching curve on which the real part of an eigenvalue is zero, that is, stability is just lost. At $\tau_1 = \tau_1^A$, the corresponding value of τ_1 jumps up to the y-value of point A. Notice that HR's stability condition is satisfied in the small solid rectangular and is strictly below the curve. Since $\cos\omega\tau_2 > 0$ and $\sin\omega\tau_2 < 0$ for $\tau_1 \in (\tau_1^A, \tau_1^B)$ and $\cos\omega\tau_1 < 0$ and $\sin\omega\tau_1 < 0$ for $\tau_1 \in (\tau_1^B, \tau_1^C)$,

$$\tau_2^B(\tau_1) = \tau_2^C(\tau_1) = \frac{1}{\omega_0}\left[2\pi - \cos^{-1}\left(\frac{N_3}{D_3}\right)\right]$$

where $\tau_2^B(\tau_1)$ for $\tau_1 \in (\tau_1^A, \tau_1^B)$ describes the blue segment between A and B whereas $\tau_2^C(\tau_1)$ for $\tau_1 \in (\tau_1^B, \tau_1^C)$ describes the magenta segment between B and C. Further $\cos\omega\tau_1 < 0$ and $\sin\omega\tau_1 > 0$ for $\tau_1 \in (\tau_1^C, \tau_1^D)$ and $\cos\omega\tau_1 > 0$ and $\sin\omega\tau_1 > 0$ for $\tau_1 \in (\tau_1^D, 2\pi)$ presents the form of

$$\tau_2^D(\tau_1) = \tau_2^E(\tau_1) = \frac{1}{\omega_0}\cos^{-1}\left(\frac{N_3}{D_3}\right)$$

where $\tau_2^D(\tau_1)$ for $\tau_1 \in (\tau_1^C, \tau_1^D)$ describes the orange segment between C and D whereas $\tau_2^E(\tau_1)$ for $\tau_1 \in (\tau_1^D, 2\pi)$ describes the green segment between D and E. Finally,

$$\tau_2^{A'}(\tau_1) = \frac{1}{\omega_0}\left[\cos^{-1}\left(\frac{N_3}{D_3}\right) + 2\pi\right]$$

describes the red segment that shifts the $\tau_2^A(\tau_1)$ curve upward with 2π and the right most red curve is described by $\tau_2^A(\tau_1)$ for $\tau_1 \in (2\pi,\ 9.80)$. It is to be noticed that the y-value of point E is

$\tau_2^E = \tau_2^A(2\pi)$. On the winding downward-sloping curve located above-rightward of the stability switching curve, one of the eigenvalues is purely imaginary but the equilibrium is already unstable there and no stability switch occurs.

Theorem 5 *The stability switching curve of dynamic system* (25) *is described by*

$$\tau_2^A(\tau_1) = \frac{1}{\omega_0}\cos^{-1}\left(\frac{N_3}{D_3}\right) \text{ for } \tau_1 \in (0, \tau_1^A).$$

To compare the stability switching curve of Model I with that of Model III, we enlarge the lower-left corner of Figure 3(A) and put the red stability switching curve (31) on the black stability switching curve of Model I in Figure 3(B). Due to the different shapes of these two curves, the region of (τ_1, τ_2) is divided into five subregions. Both models are stable in region labelled by $[S]$ and unstable in region $[U]$, indicating that roughly speaking, the delays make the equilibrium unstable when their lengths are relatively large and do not affect stability when they are smaller. Furthermore, with careful observations, we can see the following different roles of the information delays depending on the relative magnitude of the implementation delays although the information delays alone are harmless according to Theorem 4:

(i) Destabilizing role: In region $[A]$, Model I with information delays is unstable and Model III with no information delays is stable, implying that the information delays destabilize Model I when τ_1 and τ_2 are *symmetric* in the sense that they have similar values.

(ii) Stabilizing role: On the other hand, in regions $[B_1]$ and $[B_2]$, Model I is stable and Model III is unstable, implying that the information delays stabilize Model I when τ_1 and τ_2 are *asymmetric* in the sense that one of them takes a larger value and the other smaller value.

We summarize these results as follows:

Proposition 1 *When the dynamical system* (5) *has both of the implementation and information delays, the information delays become destabilizers when both delays take similar values and stabilizers when they have different values.*

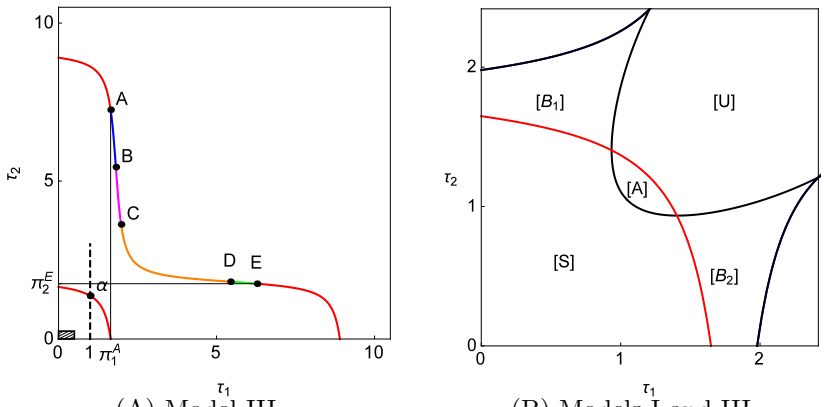

(A) Model III (B) Models I and III

Figure 3. Stability switching curves

3 Numerical Simulations

So far we have imposed the identical coefficient assumption of $k_1 = k_2$ on the output adjustment process and confine attention to a small neighborhood of the equilibrium point. In this section we modify the dynamic equations and numerically confirm the theoretical results obtained. To this end, we first introduce some nonlinearities into Models I and III to examine global behavior. Second, we take away the assumption of identical speeds of adjustment (i.e., Assumption 2) and then consider how the non-identical coefficients affect the shape of the stability switching curves and the resultant dynamics.

3.1 Global Dynamics

Since the corresponding nonhomogeneous systems of (5) and (25) are still linear, trajectories generated by these systems are divergent when the systems are locally unstable. To avoid such uninteresting and unrealistic dynamics, we introduce some nonlinearities and see the effects caused by the delays on global dynamics. The nonlinearity that we consider comes from an idea of a flexible adjustment, that is, the output adjustment responds positively to the gap between the optimal and actual outputs and the degree of responsiveness depends on the level of output in the following way,

$$K_i(x_i) = k_i \left[a_2 \left(\frac{a_1 + a_2}{a_1 e^{-(x_i - x_i^*)} + a_2} - 1 \right) + 1 \right].$$

It can be checked that

$$K_i(x_i^*) = k_i, \ \lim_{x_i \to \infty} K_i(x_i) = k_i (1 + a_1) \ \text{ and } \ K_i(0) = k_i \left[\frac{a_2 (a_1 + a_2)}{a_1 e^{x_i^*} + a_2} + 1 - a_2 \right] > 0$$

where $a_1 = 1$ and $a_2 = 1$ are assumed in the following numerical simulations.

Model I is now nonlinearized as

$$\begin{aligned} \frac{dx_1}{dt} &= K_1 [x_1(t)] [-x_1(t - \tau_1) - \beta_1 x_2(t - \tau_1) + \alpha_1], \\ \frac{dx_2}{dt} &= K_2 [x_2(t)] [-\beta_2 x_1(t - \tau_2) - x_2(t - \tau_2) + \alpha_2], \end{aligned} \tag{32}$$

both of which can be reduced to (5) by linear approximation in the neighborhood of the equilibrium point.[4] We perform two simulations. In the first simulation, we choose τ_2 as a bifurcation

[4] To do output adjustment in system (32), the firms do not need the current output values and the derivatives $\dot{x}_1(t)$ and $\dot{x}_2(t)$. The following method can be used. Rewrite the equations as

$$\frac{\dot{x}_i(t)}{x_i(t)} = K_i [-x_i(t - \tau_i) - \beta_i x_j(t - \tau_i) + \alpha_i] \ \text{ for } i = 1, 2 \text{ and } j \neq i$$

and integrating both sides in interval $[0, t]$

$$\ln[x_i(t)] = \ln[x_i(0)] + K_i \int_0^t [-x_i(s - \tau_i) - \beta_i x_j(s - \tau_i) + \alpha_i] \, ds$$

showing that to obtain $x_i(t)$ only delayed output values are needed. In the more general case of equations

$$\dot{x}_i(t) = f [x_i(t)] [-x_i(t - \tau_i) - \beta_i x_j(t - \tau_i) + \alpha_i] \ \text{ for } i = 1, 2 \text{ and } j \neq i$$

numerical methods such as the Euler method or any higher oder Runge-Kutta type method can be used, which gives the output values, $x_i(0)$, $x_i(h)$, $x_i(2h)$, ...with a step size h and at each step only earlier output values are used (see for example, Szidarovszky and Yakowitz, 1978). Here τ_1 and τ_2 have to be integer multiples of h, otherwise the values of $x_i(t - \tau_i)$ and $x_j(t - \tau_j)$ are obtained by interpolation. Bischi et al. (2010) introduced this general output adjusting form with sign-preserving speeds of adjustments.

parameter and increase the value of τ_2 from 0 to 5 with an increment of 0.01 along the vertical dotted line at $\tau_1 = \pi/3 \simeq 1.05$ in Figure 2. For each value of τ_2, the fully delayed system (32) is simulated for $0 \leq t \leq 1000$. We generate 1000 data of $x_2(t)$ from the solutions for $t \in [900, 1000]$ by changing t with an increment of 0.1 and then plot the local maximum and minimum out of the data vertically just above the point τ_2, to illustrate the corresponding bifurcation diagram with respect to τ_2 in Figure 4(A). The vertical line at $\tau_1 = \pi/3$ passes through the point at which the orange and green curve are connected (i.e., $\tau_2^a = \pi/3$), crosses the orange curve at $\tau_2^b \simeq 2.02$ and then crosses the black curve at $\tau_2^c \simeq 2.28$. Figure 4(A) indicates that the equilibrium point is stable for $\tau_2 < \tau_2^a$ and loses stability at the first intersection at point $a = (\pi/3, \tau_2^a)$. The equilibrium point bifurcates to a limit cycle for $\tau_2 \in (\tau_2^a, \tau_2^b)$ and then regains stability when it arrives at the second intersection $(\pi/3, \tau_2^b)$.[5] For further increases of τ_2 the system loses stability again at $(\pi/3, \tau_2^c)$ and the corresponding bifurcation gets a bit complicated. In particular, a limit cycle with two extremum (one maximal and one minimal) emerges first and then it turns to be a cycle with four extremum that then becomes the one with six extremum and so on. The system does not regain stability for values of τ_2 larger than τ_2^c.

In the second simulation, we change the value of τ_1 to $4\pi/3\sqrt{3} \simeq 2.42$ and repeat the same procedure to obtain the bifurcation diagram illustrated in Figure 4(B). The starting point $(4\pi/3\sqrt{3}, 0)$ is located in the region to the right of the lower black curve in Figure 2, the equilibrium point is locally unstable and Figure 4(B) indicates the birth of a limit cycle at this point. As the value of τ_2 increases along the vertical dotted line at $\tau_1 = 4\pi/3\sqrt{3}$, the corresponding limit cycle gradually shrinks and discontinuously jumps to a different limit cycle at point $(4\pi/3\sqrt{3}, \tau_2^a)$ where $\tau_2^a = 2\pi/3\sqrt{3} \simeq 1.21$. Further increasing τ_2 leads to complicated dynamics through a period-doubling cascade. Notice that τ_i has exactly the same effect as τ_j as the stability switching curve is symmetric with respect to the diagonal. These numerical results are summarized as follow: In the dynamic process of nonlinearized Model I, (1) the delay has the dual roles of destabilizer and stabilizer according to its length when the stationary state is locally stable at the starting point and (2) increasing a value of delay can generate complex dynamics involving chaotic behavior when the stationary state is locally unstable at the starting point.

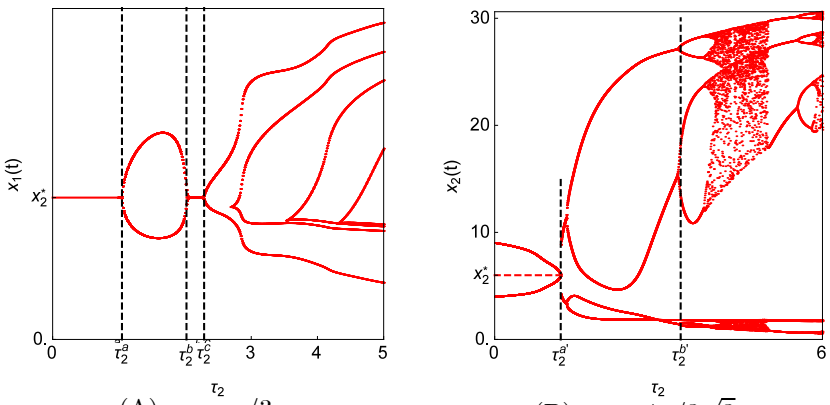

(A) $\tau_1 = \pi/3$ (B) $\tau_1 = 4\pi/3\sqrt{3}$

Figure 4. Bifurcation diagrams of the nonlinear Model I

[5] It is possible to determine directions of the stability switch analytically. See Lin and Wang (2012) for theoretical foundation and Matsumoto and Szidarovszky (2015) for its application.

We now turn attention to the nonlinearized Model III,

$$\frac{dx_1}{dt} = K_1\left[x_1(t)\right]\left[-x_1(t-\tau_1) - \beta_1 x_2(t) + \alpha_1\right],$$

$$\frac{dx_2}{dt} = K_2\left[x_2(t)\right]\left[-\beta_2 x_1(t) - x_2(t-\tau_2) + \alpha_2\right].$$

Two simulations are performed for the new Model III.[6] The first simulation is presented in Figure 5(A) in which the value of τ_2 increases from 0 to 3 along the vertical dotted line at $\tau_1 = 1$ in Figure 3(A). The system is asymptotically stable for the starting point of $\tau_1 = 1$ and $\tau_2 = 0$ and remains stable until point $(1, \tau_2^A)$ where point a is on the stability switching curve in Figure 3(A). As is seen, at a critical value τ_2^A, the stationary state loses stability and bifurcates to a limit cycle. Notice that the stability regain does not occur and thus the delay does not have the dual roles. As seen in Figure 4(A), making τ_2 larger than the critical value of τ_2^A increases the number of extremum of the limit cycle. In the second simulation, we change the fixed value of τ_1 to 2 and repeat the same procedure. However, to avoid graphical congestion of Figure 3(A), the line at $\tau_1 = 2$ is not illustrated. The resultant dynamics illustrated in Figure 5(B) in which the system is unstable and its dynamic behavior gets complicated as τ_2 increases, that is, we alternatively have windows for complex dynamics and the one for a periodic limit cycle.

Proposition 2 *In the dynamic process of nonlinearized Model III, (1) stability is lost at $\tau_2 = \tau_2^A$ and never regained since the delay crosses the stability switching curves only once when the stationary state is stable at the starting point; (2) as τ_2 increases, dynamics alternates between complicated behavior and periodic cyclic behavior with increasing the periodic number.*

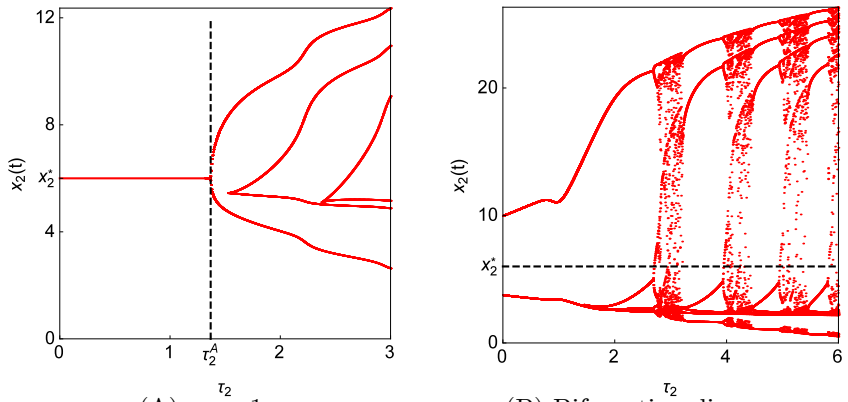

(A) $\tau_1 = 1$ (B) Bifurcation diagram

Figure 5. Bifurcation diagrams of the nonlinear Model III

3.2 Non-Identical Coefficients

We now use the non-identical adjustment coefficients to see how such asymmetry affects the results obtained. We have already shown that the stability switching curves in Case I (that is, the black curves in Figure 2) can be constructed only under the symmetry Assumption 2. It is

[6] Matsumoto and Szidarovszky (2015) also consider dynamics of a delay nonlinear model of Cournot duopoly having the similar structure. However the growth rate of outputs is determined by a product of the marginal profit and an adjustment function depending on the level of output. As a natural consequence of the different adjustment process, it has different dynamic behavior.

expected that the stability switching curves obtained in Case II may be distorted. In order to illustrate the effect of different speeds of adjustment, we present numerical simulations concerning the shape of the stability switching curves and the dynamics of the nonlinearized Model I. The values of the coefficients are $k_1 = 3/2$ and $k_2 = 1$ in the first simulation and are changed to $k_1 = 1/2$ and $k_2 = 1$ in the second.

In the first simulation, solving $F(\omega) = 0$ determines the interval $\Omega = [\omega_3, \omega_1] \cup [\omega_2, \omega_4]$ where

$$\omega_3 \simeq 0.589,\ \omega_1 \simeq 0.840,\ \omega_2 \simeq 1.340,\ \omega_4 \simeq 1.911.$$

Notice that $\omega_1 \neq \omega_2$ when $k_1 \neq k_2$. In Figure 6(A) stability switching curves are illustrated as solid curves in the same color as in Figure 2, that is, the blue curve is described by $\left(\tau^+_{1,0}(\omega),\ \tau^-_{2,1}(\omega)\right)$ for $\omega \in [\omega_3, \omega_1]$ and the red curve exists outside the designated region whereas the green and orange curves are given by $\left(\tau^+_{1,1}(\omega),\ \tau^-_{2,1}(\omega)\right)$ and $\left(\tau^-_{1,1}(\omega),\ \tau^+_{2,1}(\omega)\right)$ for $\omega \in [\omega_2, \omega_4]$ and they end at the same point $(\tau^*_1(\omega_4), \tau^*_2(\omega_4))$.[7] The nonlinear system (32) is asymptotically stable in the lower-left region surrounded by these curves. It is seen that the shaded rectangular, HR's stability region, is still inside it. The stability switching curves with $k_1 = k_2 = 1$ are also illustrated as the dotted curves in the same color. Comparing the new stability region with the old one reveals that the asymmetric coefficients shift the solid orange curve leftward and the solid green curve downward, resulting in a shrink of the stability region. On the other hand, a part of the solid blue curve is located above the dotted black curve, indicating an enlargement of the stability region. As far as the current example is concerned, the increase seems to be larger than the decrease. Thus the stability region becomes smaller. It is not sure if this result is specific or general. The bifurcation diagram with respect to τ_2 in Figure 6(B) is constructed along the vertical dotted line at $\tau_1 = \tau^*_1(\omega_4)$. The vertical line intersects these stability switching curves three times at the following values of τ_2,

$$\tau^a_2 \simeq 0.822,\ \tau^b_2 \simeq 1.325 \text{ and } \tau^c_2 \simeq 2.36$$

which are at the connecting point of the green and orange curves, on the orange curve and on the blue curve, respectively. Stability is lost at $\tau_2 = \tau^a_2$ and regained at $\tau_2 = \tau^b_2$ while a limit cycle is born for $\tau_2 \in (\tau^a_2, \tau^b_2)$. Stability is lost again at $\tau_2 = \tau^c_2$ and not regained for any $\tau_2 > \tau^c_2$. The diagram indicates that a limit cycle becomes more distorted as the value of τ_2 is getting larger.

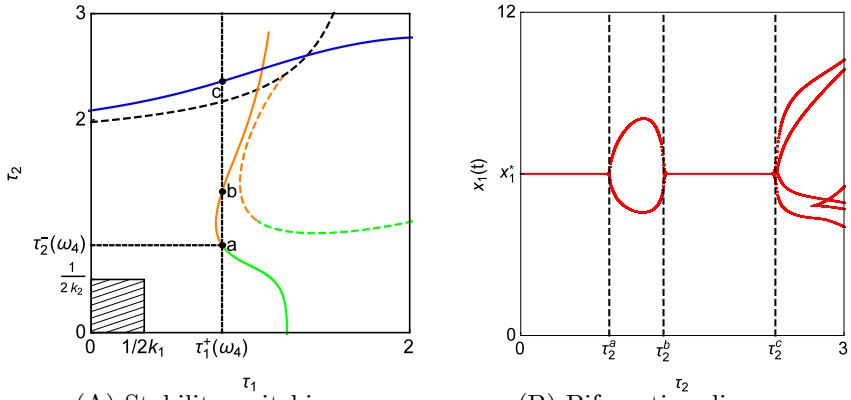

(A) Stability switching (B) Bifurcation diagram

Figure 6. $k_1 = 1.5$ and $k_2 = 1$

In the second simulation, the different value of k_1 presents different solutions for $F(\omega) = 0$,

$$\omega_3 \simeq 0.317,\ \omega_1 \simeq 0.411,\ \omega_2 \simeq 0.911,\ \omega_4 \simeq 1.183.$$

[7] Needless to say, $\tau^*_1(\omega_4) = \tau^+_{1,1}(\omega_4) = \tau^-_{1,1}(\omega_4)$ and $\tau^*_2(\omega_4) = \tau^-_{2,1}(\omega_4) = \tau^+_{2,1}(\omega_4)$.

In Figure 7(A) the red curve is described by $\left(\tau_{1,1}^{-}(\omega),\ \tau_{1,0}^{+}(\omega)\right)$ for $\omega \in [\omega_3, \omega_1]$ and the region surrounded by the orange, green and red curves is the stability region that includes the shaded rectangular region. As in Figure 6(A), the stability switching curves with $k_1 = k_2 = 1$ are illustrated as the dotted curves in the same color. It is seen that decreasing the value of k_1 shifts the solid green curve upward and makes the slope of the solid orange curve flatter. As a result, the stability region is increased in one part and decreased in the other part. In the current example, the stability region becomes larger. The bifurcation diagram with respect to τ_1 in Figure 7(B) illustrates the change of dynamical behavior of the nonlinearized Model I as the length of the delay τ_1 is varied along the horizontal dotted line at $\tau_2 = \tau_2^*(\omega_4)$. It is observed that the bifurcation diagram in Figure 7(B) is similar to the diagrams in 6(B). In particular, stability is lost at $\tau_1 = \tau_1^a$ and regained at $\tau_1 = \tau_1^b$ whereas a limit cycle emerges for $\tau_1 \in (\tau_1^a, \tau_1^b)$. It is lost again at $\tau_1 = \tau_1^c$. and never regained for any $\tau_1 > \tau_1^c$. A limit cycle emerges for $\tau_1 > \tau_1^c$ and becomes larger with increasing the number of the extrema as τ_1 gets larger than τ_1^c.

We summarize the effect caused by different coefficients: Non-identical coefficients of k_1 and k_2 change the shape of the stability switching curve and it depends on the relative magnitude of the coefficients whether the stability region becomes larger or smaller.

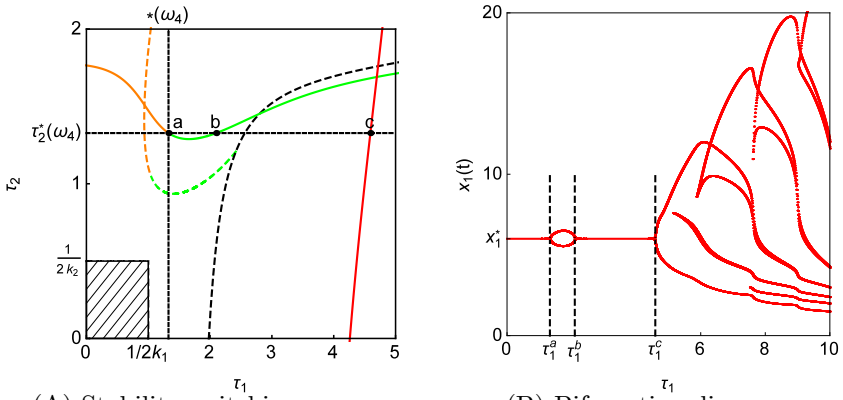

(A) Stability switching curve (B) Bifurcation diagram

Figure 7. $k_1 = 0.5$ and $k_2 = 1$

4 Concluding Remarks

In this paper we have analyzed the dynamics of three different types of the Cournot duopoly model with multiple discrete delays, Model I with the implementation and information delays, Model II with only the information delays and Model III only with the implementation delays. For stability analysis, we adopted the linear models that were used by HR and constructed the stability switching curve on which stability was lost or gained. For global dynamics, we nonlinearized the models and performed numerical simulations. In doing so, we demonstrated three main results:

(i) In Model I, the delays has the dual roles of destabilizer and stabilizer and complicated dynamics involving chaotic behavior can emerge for larger values of the delays.

(ii) In Model II, the information delays alone do not affect stability.

(iii) In Model III, the implementation delays can destabilize the otherwise stable stationary state, however, they do not have the dual roles.

Acknowledgement: The second author highly acknowledges the financial supports from the MEXT-Supported Program for the Strategic Research Foundation at Private Universities 2013-2017, the Japan Society for the Promotion of Science (Grant-in-Aid for Scientific Research (C) 16K03556) and Chuo University (Joint Research Grant).

References

[1] Bischi, G. I., Chiarella, C., Kopel, M. and Szidarovszky, F., *Nonlinear oligopolies: stability and bifurcations*, Heidelberg, Dordrecht/London/New York, Springer, 2010.

[2] Cooke, K. L. and Grossman, Z., Discrete delay, distributed delay and stability switches, *Journal of Mathematical Analysis and Applications*, 86, 592-627, 1982.

[3] Cournot, A., *Recherches sur les Principes Mathématiques de la Théorie des Richessess*, Paris, Hachette, 1838 (Englich translation: *Researches into the Mathematical Principles of the Theory of Wealth*, New York, Kelley, 1960).

[4] Fisher, F., The stability of the Cournot solution: the effects of speeds of adjustment and increasing marginal costs, *Review of Economic Studies*, 28, 125-135, 1961.

[5] Gori, L, Guerrini, L. and Sodini, M., Disequilibrium dynamics in a Keynesian model with time delays, *Communications in Nonlinear Science and Numerical Simulations*, 58, 119-130, 2018.

[6] Gori, L, Guerrini, L. and Sodini, M., A characteristic of duopoly dynamics with frictions in production adjustments, *Journal of Evolutionary Economics*, 27, 963-988, 2017.

[7] Gori, L, Guerrini, L. and Sodini, M., A continuous time Cournot duopoly with delays, *Chaos, Solitons and Fractals*, 79, 166-177, 2015.

[8] Gu, K., Niculescu, S. and Chen, J., On stability crossing curves for general systems with two delays, *Journal of Mathematical Analysis and Applications*, 311, 231-252, 2005.

[9] Hahn, F., The stability of the Cournot oligopoly solution, *Review of Economic Studies*, 29, 329-331, 1962.

[10] Howroyd, T. D. and Russel, A. M., Cournot oligopoly models with time delays, *Journal of Mathematical Economics,* 13, 97-108, 1984.

[11] Lin, X. and Wang, H., Stability analysis of delay differential equations with two discrete delays, *Canadian Applied Mathematics Quarterly*, 20, 519-133, 2012.

[12] McManus, M. and Quandt, R., Equilibrium numbers and size in Cournot oligopoly, *Yorkshire Bulletin of Social Science and Economic Research*, 16, 68-75, 1964.

[13] Matsumoto, A., Merlone, U. and Szidarovszky, F., Goodwin accelerator model revisited with fixed time delays, *Communications in Nonlinear Science and Numerical Simulations*, 58, 233-248, 2018.

[14] Matsumoto, A., Szidarovszky, F., and Asada, T. (ed.), *Essays in Economic Dynamics: Theory, Simulation Analysis and Methodological Study*, Berlin/Tokyo, Springer, 2016.

[15] Matsumoto, A. and Szidarovszky, F., Nonlinear Cournot duopoly with implementation delays, *Chaos, Solitions and Fractals*, 79, 157-165, 2015.

[16] Okuguchi, K., *Expectations and Stability in Oligopoly Models*, Berlin, Springer, 1976.

[17] Okuguchi, K. and Szidarovszky, F., *The Theory of Oligopoly with Multi-product Firms*, 2nd edition, Berlin, Springer, 1999.

[18] Szidarovszky, F. and Yakowitz, S., *Principles and Procedures of Numerical Analysis*, New York, Plenum Press, 1978.

[19] Theocharis, R. D., On the stability of the Cournot solution on the oligopoly problem, *Review of Economic Studies*, 27, 133-134, 1960.